catalysts

MDPI

Article

Improved Hydrothermal Stability in Glass Diesel Soot Oxidation Catalysts

James Zokoe [1], Xiaoxiang Feng [2], Changsheng Su [1] and Paul J. McGinn [2,*]

[1] Cummins Inc., 1900 McKinley Ave., Columbus, IN 47201, USA
[2] Department of Chemical and Biomolecular Engineering; University of Notre Dame, Notre Dame, IN 46556, USA
* Correspondence: pmcginn@nd.edu; Tel.: +574-631-6151

Received: 26 July 2019; Accepted: 8 August 2019; Published: 13 August 2019

Abstract: The hydrothermal stability of K-Ca-Si-O glass soot oxidation catalysts has been improved by substitution of Ce and Zr for Ca. This work demonstrates that glasses can be tailored to withstand the challenging diesel exhaust hydrothermal environment by considering the field strengths and partial molar free energies of the hydration reactions (ΔG_i) of the cation species in the glass. The result is a glass that shows less formation of precipitates after 2 h hydrothermal exposure in air with 7% H_2O at temperatures ranging from 300–700 °C. A K-Ca-Si-O glass with a soot T_{50} (the temperature when 50% of the soot is oxidized) of 394 °C was found to degrade to 468 °C after a 2 h, 700 °C hydrothermal exposure, whereas the improved K-Ce-Zr-Si-O glass only changed from 407 °C to 427 °C after the same treatment.

Keywords: soot oxidation; potassium catalyst; glass catalyst; diesel particulate filter; glass weathering; glass corrosion

1. Introduction

A diesel particulate filter (DPF) is used to remove harmful soot particles from the exhaust stream of a diesel engine. With extended use, soot accumulates in the filter and must be removed to avoid a large pressure drop in the exhaust system and maintain efficiency. So-called active filter regeneration is accomplished by raising the temperature to a sufficiently high value (550–600 °C) to allow soot oxidation. There is interest in developing low cost catalysts that can lower the temperature required for soot oxidation, as well as increase its selectivity to CO_2 [1]. In particular, non-noble metal catalysts are of great interest in this regard. Many catalyst formulations have been studied for the purpose of enhancing soot combustion. Alkali containing compounds are among those that have shown promise by exhibiting low oxidation temperatures, with potassium-based compounds being the subject of many investigations [2–12].

Although it is well known that potassium is among the most active carbon oxidation catalysts, the mechanistic role of K is not yet clear, and a large number of postulated mechanisms are described in the literature, as have been recently reviewed [13]. For example, it has been suggested that potassium can increase chemisorbed oxygen [14,15], that K^+ species activate oxygen to form a ketene intermediate that is further oxidized to CO_2 [16], or that potassium facilitates the interaction between catalyst and soot due to high mobility, thus resulting in good activity [17]. The high mobility is also suggested to be responsible for the rapid degradation of potassium-based catalysts during the oxidation process due to sublimation losses [18,19]. Use of potassium for diesel soot oxidation requires that its mobility be accounted for in order to prolong the catalytic activity to be compatible with the lifetime of the emissions reduction unit.

To overcome potassium loss issues, many researchers have tried to stabilize the K ions by binding the element to a support [20–22]. Increased stabilization of potassium can be achieved in compounds such as perovskite- and spinel-type oxides [5,23–25] or mixed transition metal oxides [26–28]. Strong bonding between the K^+ and a host compound or the substrate can hinder the mobility of the ion and therefore slow degradation of the catalyst due to loss of potassium. The disadvantage of this method is that catalytic activity can also be hindered by diminished mobility. The challenge in using potassium compounds is the need to balance between activity and stability (i.e., recognizing that enhanced activity through catalytic mobility potentially will increase the K loss rate) [8].

An approach to balance between activity and stability in K-based catalysts developed in our lab uses a silica glass in which the K^+ ions present within the silicate matrix act as a catalyst [29–32]. When the glass is exposed to water vapor, such as in diesel exhaust, ion exchange of H^+ and potassium ions can occur. This causes migration of K^+ to the glass catalyst surface and provides a continuous supply of potassium for catalytic soot combustion over long times. The composition of the glass can be tuned to balance both glass degradation and catalytic activity by the incorporation of network strengthening elements [33]. The specifics of this methodology will be discussed in a more detail below. By optimizing the glass composition, soot combustion temperatures in the 375–400 °C range have been achieved with this novel catalyst.

Although alkali based catalysts show promise they are not yet commercially viable as a long life catalyst in diesel applications, as they have not demonstrated activity over multiple combustion cycles or temperature excursions above 600 °C [34,35]. The focus of the present study is to document hydrothermal damage in a glass diesel soot oxidation catalyst and show how composition modifications can be used to mitigate the deterioration.

A DPF catalyst, glass or otherwise, must survive the harsh conditions of the diesel exhaust environment for extended periods of time. This means the catalyst must have appropriate resistance to structural changes caused by elevated temperatures and hydrothermal exposure. Glass degradation can be classified as chemical or structural in nature [36]. Within these two categories there exist various degradation mechanisms pertinent to a diesel exhaust environment. Although only a handful of reports describe the use of glasses in a diesel exhaust environment, the degradation of glass has been widely studied in the fields of nuclear waste storage and the preservation of glass artifacts [37–39].

A physical crust can develop on a glass surface due to extensive leaching and re-precipitation of mobile elements. As described by Newton [40], and recently extensively tested by Melcher et al. [39] and Gentaz et al. [41], potash and lime containing glasses when exposed to atmospheric gases such as SO_2, NO_x, and CO_2 will form a 'weathering' crust of sulfates, nitrates, and carbonates, respectively. This crust can become a barrier to further ion leaching and the structural reformation at the surface can reach a limiting thickness, which is dependent upon factors including glass composition, atmospheric gas composition, and exposure time. A glass exposed to diesel exhaust will experience a similar environment of acidifying gases but the high flow rate of exhaust and the elevated temperatures can be expected to greatly accelerate the weathering process. However, the presence of soot and soot combustion on the surface may alter the development of a surface crust by consuming K that would otherwise accumulate at the surface [22,42,43]. In fact, the presence of a soot layer has been shown to slow degradation in catalytic activity of a glass catalyst [32].

In most applications glass degradation is to be avoided. For example, glasses for storage of nuclear waste are expected to be stable over thousands of years. However, for biological or diesel catalysis applications controlled glass degradation is desired. The effect of glass constituents on durability can be predicted by considering a glass as a mixture of species with known free energies of hydration [44]. The degradation of a glass can be scaled as the sum of the free energies of hydration of the individual glass components ($\Delta G_{(hydration)i}$) as silicates or oxides relative to their respective molar fraction (x_i) [45]. Equation (1) illustrates this simple idea.

$$\Delta G_{(hydration)} = \sum_i x_i * \Delta G_{(hydration)i} \quad (1)$$

To design durable glasses, glass reactant species are selected based on hydration reactions that are anticipated to occur between the glass and an aqueous solution (acidic or basic). This is based on expectations as to whether cations in the glass will anionically complex with silica or other oxides, which is determined from their relative anionic force, reflecting their relative field strength (F). Network formers are ions with high atomic field strengths (F), (calculated as the atomic charge (Z) divided by the square of the ionic radius (r)), while network modifiers are ions with low atomic field strengths. Potassium and sodium are examples of network modifiers that have low field strengths, so are susceptible to leaching. Network modifier cations are oxide species which are highly anionically associated with $[SiO_4]^{-4}$ tetrahedra, such as $K_2O + SiO_2$. The field strengths are considered along with the relative partial molar free energies of the hydration reactions (ΔG_i) of the cation species that can occur in an aqueous environment. Figure 1 shows the range of hydration energies for common glass additives versus their respective ionic field strength (F).

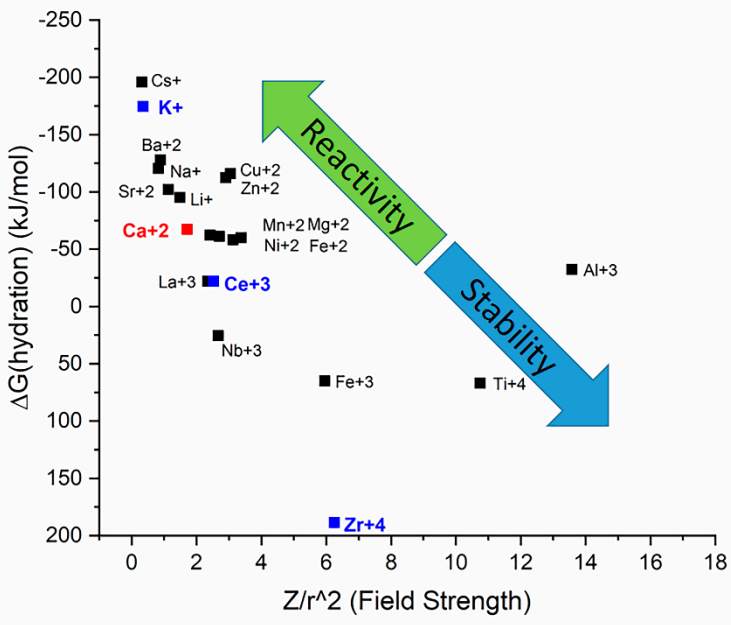

Figure 1. Gibbs free energy of hydration of glass additives relative to their ionic field strengths.

The addition of low field strength, highly negative free energy of hydration elements will cause greater susceptibility to chemical degradation due to increased leaching of these elements from the glass. A hydrated, depleted surface results from the leaching and extends further into the surface with longer exposure times. The growth of this hydrated layer is governed by a square root dependence with respect to time since the growth of the surface layer eventually impedes further leaching through the depleted zone [37,44,45].

For example, for the case of a simple potassium silicate glass, Figure 1 suggests that the addition of Al will to create a more chemically durable glass than a glass with equivalent Ca additions due to the overall increase in free energy of hydration and ionic potential. Specifically, the isomorphic substitution of Al for Si into the glass network brings an additional negative charge increasing the bonding strength of the K^+ which locally associates with the negative charge. Thus, an overall increase in the resistance to ion mobility is gained through the structural incorporation of Al compared to Ca. For catalytic glasses, this type of compositional tuning can be used to strike a balance between durability (achieved through slow ionic movement) and catalytic activity (preferring easy ionic mobility) [33].

In an earlier study the degradation of a K-Ca-Si-O glass in a hydrothermal environment analogous to that encountered in diesel exhaust was documented [31]. In that work partial catalytic deactivation was determined to be caused by $CaCO_3$ formation on the surface after prolonged exposure to humid

gas. Ca compounds show minimal activity in carbon oxidation [46,47] so their presence of the glass surface reduces the catalytically active area.

Replacing the Ca in the K-glass composition with another stabilizing element that also is catalytically active in soot oxidation could improve the useful lifetime performance of the glass catalyst. Based on the ionic field strength reasoning described above, one expects improved glass stability (reduced corrosion) with ZrO_2 additions. This has been shown to be the case in several studies [48,49]. However, recent reports suggest that small additions of ZrO_2 to silica glass lead to an increase in corrosion [50,51]. At low doping levels (0.4–2 mol%) it was found that because ZrO_2 is less soluble than Si, it slows leaching kinetics as expected, but simultaneously it hinders structural reorganization at the surface. This hindrance has the effect of keeping the structure open, thereby allowing corrosion to continue. Hence, although it is well established that high levels of Zr additions enhance glass stability, there is a maximum in the corrosion rate with low level ZrO_2 additions. For a catalytic glass such a mechanism could be a source of control for catalyst leaching to prevent a thick protective crust from forming and deactivating catalytic activity. Additions of Zr to a K-glass catalyst could allow replenishment of K^+ ions to the surface during K depletion events, such as soot oxidation with reduced humidity, by forcing the silicate structure to remain open, effectively allowing better use of the sub-surface K.

Additionally, Ce replacement of Ca could prove beneficial, as CeO_2 has shown significant oxygen storage capacity, which aids in catalytic oxidation of soot [52–55]. Cerium as a glass constituent acts as a stronger network former than Ca, due a higher $\Delta G_{hydration}$ of −22.0 kJ/mol [37]. Complete substitution of Ce for Ca in the K-glass composition could negate any catalytic degradation due to inactive species on the surface. Moreover, a higher amount of K could be stabilized in the glass since the Ce free energy of hydration is less negative than Ca [45]. Additional K in the catalyst should promote more efficient replenishment of the surface to compensate for any loss of K due to sublimation during soot oxidation. In this research we examine the effects of modifying a simple potassium calcium silicate glass through Ce and Zr substitutions to achieve improved hydrothermal stability.

2. Results and Discussion

2.1. Catalytic Activity Characterization by HR-TGA

TGA characterization of the powder samples was used as a first comparative screening parameter for the compounds. The characteristic T_{ig} and T_{50} values are shown in Table 1. All three KCeZr compositions performed on par with the KCS-1 catalyst.

Table 1. T_{IG} and T_{50} values of investigated glass compositions.

Composition	Contact Condition			
	Tight		Loose	
	T_{ig}	T_{50}	Tig	T_{50}
KCS-1	367.16	376.29	382.76	405.06
KCeZr-1	365.1	372.36	395.91	410.67
KCeZr-2	363.72	370.81	392.8	402.32
KCeZr-3	369.79	374.21	399.18	411.23

Small additions of Zr to the KCS-1 glass composition could improve the chemical durability of a K-Ca-Si-O glass in a hydrothermal environment by strengthening the surface against restructuring. However, the Ca in the glass can still leach to the surface and lower the catalyst activity by forming inactive precipitates [31]. By replacing the Ca in the glass with Ce and a small amount of Zr, all three KCeSZ compositions provide nearly equivalent soot oxidation performance compared to the KCS-1 composition without the catalytically inactive Ca element. Additionally, they offer the possibility of gaining the catalytic benefit of Ce, as will be described below.

2.2. Hydrothermal Testing of KCeSZ-1 Glass Composition

Based on the TGA results, the KCeSZ-1 glass was examined in more detail. To study the chemical degradation characteristic of the KCeSZ-1 glass composition, a series of hydrothermal experiments were conducted at temperatures ranging from 300–700 °C. The hydrothermal environment was created by flowing air through a water bubbler to accumulate 7% H_2O vapor. KCS-1 and KCeSZ-1 coated cordierite samples were exposed to the synthetic hydrothermal environment for 2 h at 300, 500, 600, and 700 °C. The degree of catalytic soot oxidation degradation was characterized by soot oxidation temperatures measured by HR-TGA before and after the hydrothermal treatments in a simulated diesel exhaust atmosphere (10% O_2, 5% CO_2, 3% H_2O with balance N_2). Table 2 tabulates the corresponding T_{ig} and T_{50} soot oxidation temperatures measured for both glasses after the hydrothermal treatments.

Table 2. T_{IG} and T_{50} of KCS-1 and KCeSZ-1 coatings on cordierite after 2 h hydrothermal exposure at various temperatures.

	KCS-1		KCeSZ-1	
Hydrothermal Temperature 2 h Exposure	**Tig (°C)**	**T50 (°C)**	**Tig (°C)**	**T50 (°C)**
As-Made	388	405	390	405
300	368	380	359	384
500	387	401	388	401
600	413	430	391	406
700	425	468	410	427

For the hydrothermal treatments of 300, 500, 600, and 700 °C the measured T_{ig} temperatures for the KCeSZ-1 coated cordierite samples were 359, 388, 391, and 410 °C respectively. Comparatively, for the equivalent hydrothermal treatments, of the KCS-1 coated catalyst, the measured T_{ig} temperatures for the KCS-1 catalyst were 368, 387, 413, and 425 °C respectively. For both glasses the values after 300 and 500 °C exposure are lower than the as-made values. This is the result of the humid environment promoting ion exchange, and enriching the surface in potassium. [29] Comparatively, the KCeSZ-1 coated cordierite catalyst measured a comparable oxidation activity (~4 °C higher T_{50}) relative to the KCS-1 coated cordierite after the 300 °C hydrothermal treatment, similar activity after the 500 °C treatment, ~24 °C lower T_{50} temperature after 600 °C, and ~40 °C lower T_{50} after hydrothermal exposure at 700 °C.

Flat, polished samples of the KCeSZ-1 glass composition were created and exposed to the equivalent hydrothermal testing as the coated cordierite samples to give a sample that is easily inspected for signs of surface degradation caused by the hydrothermal environment. SEM/EDS was utilized to characterize the chemical degradation and to compare the surface of the KCeSZ-1 to the previously examined KCS-1 glass. Figure 2 shows the SEM images of the KCeSZ-1 glass after 2 h hydrothermal exposures (~7% H_2O in air) at temperatures of 300, 500, 600, and 700 °C. Figure 3 shows the comparable set of images for the KCS-1 glass.

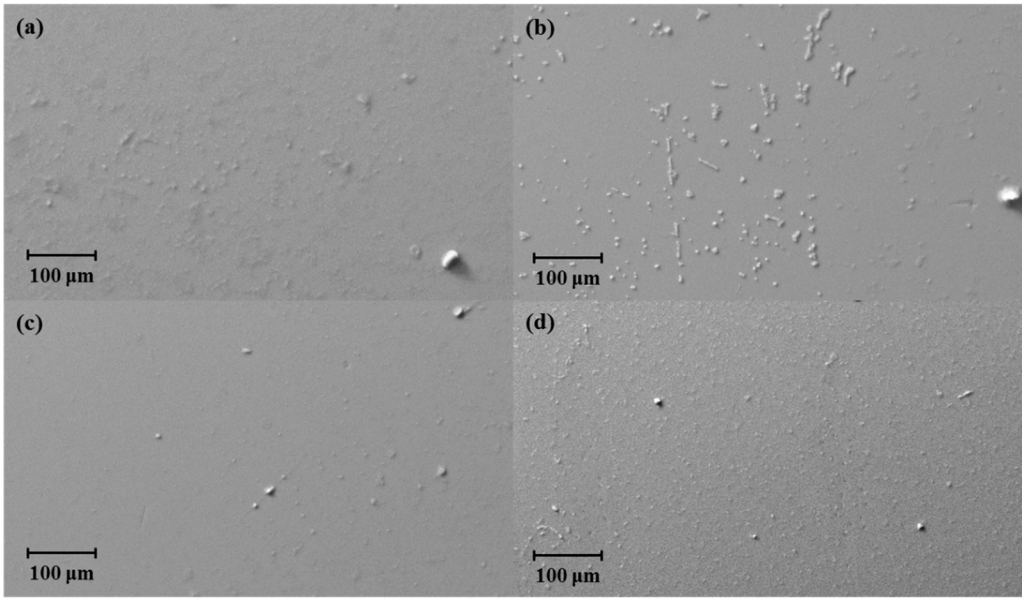

Figure 2. SEM images of polished KCeSZ-1 melt glass slices after 2 h hydrothermal exposures in air with 7% H_2O at (**a**) 300 °C, (**b**) 500 °C, (**c**) 600 °C, and (**d**) 700 °C. Separate samples were used for each testing condition.

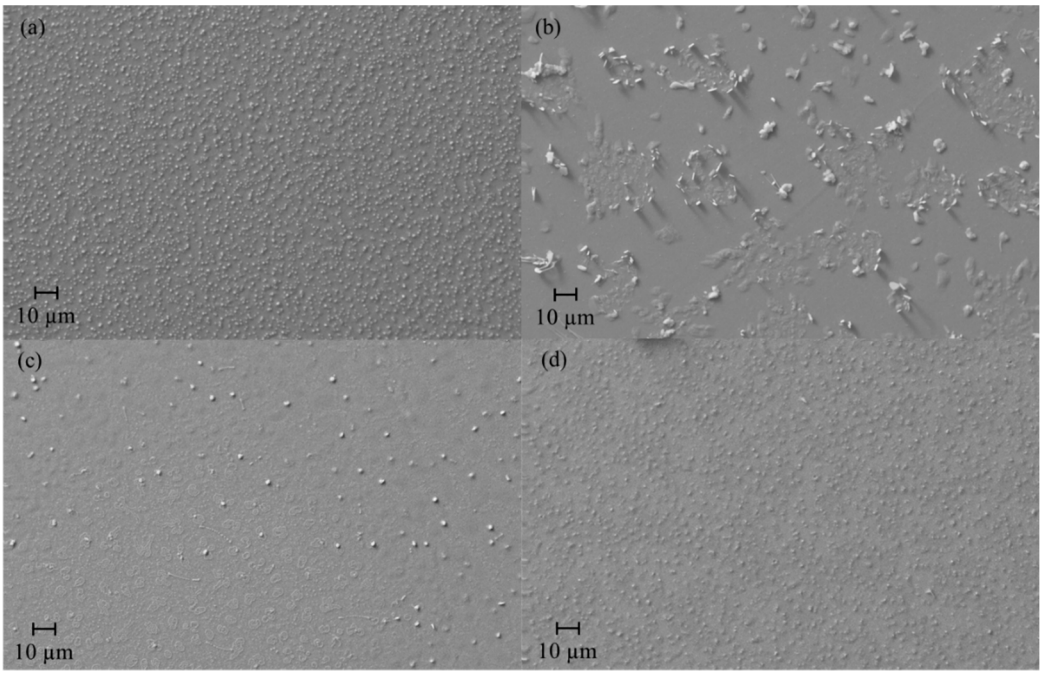

Figure 3. SEM images of polished KCS-1 melt glass slices after 2 h hydrothermal exposure in air with 7% H_2O at (**a**) 300 °C,(**b**) 500 °C, (**c**) 600 °C, and (**d**) 700 °C. Separate samples were used for each testing condition (reproduced from [31]).

For all conditions, degradation to the formerly smooth surface appears in the form of protrusions and precipitates. By comparing the sets of images, it is obvious that the KCeSZ-1 glass experienced less surface degradation than the KCS-1 glass at all temperatures. The KCeSZ-1 glass shows minimal precipitate formation at 300, 600, and 700 °C, with only small precipitates forming at 500 °C. Similar to what is seen with the KCS-1 glass composition, numerous, small precipitates nucleate on the glass surface after 700 °C hydrothermal exposure.

EDS compositional measurements were performed at higher magnification of 2.5 kX on these KCeSZ-1 glass samples hydrothermally exposed at temperatures of 300–700 °C. Table S1 shows the average compositional measurements of five point spectra of each of the precipitates and surrounding flat glass per sample. Area EDS scans of ~1 mm were also used to compare the compositional change of the near surface at the various hydrothermal treatment temperatures. Error shown is the standard deviation of the measured at.% of the five point spectra.

The resulting composition was greatly dependent on the thickness of the measured precipitates. Regardless, of the precipitates that did form on the glass surface, all precipitates measured high in potassium content relative to the surrounding flat glass. K at% in the precipitates measured a maximum of 20.4 after 500 °C hydrothermal treatment and a minimum of 14.1 after 700 °C hydrothermal exposure. The flat glass surrounding the precipitates measured values between 9.49 to 16.2 at% K corresponding to the 300 °C and 600 °C hydrothermal treatments respectively. Without including the oxygen content in the measured at% ratio, these K values correspond to 44.5 and 39.7 for the precipitates and 40.3 and 40.4 for the flat glass areas, respectively. Comparing these values to the as made KCeSZ-1 glass composition (without oxygen) of 39.5 at% K, the precipitates measured slightly higher in K content while the surrounding glass was minimally effected by the hydrothermal treatment.

The 1 mm^2 EDS area measurements showed minimal difference in composition for all hydrothermal temperatures. This further indicates the chemical resistance of the KCeSZ-1 glass composition and minimal near surface restructuring caused from the hydrothermal environment. In the KCS-1 glass, both K_2CO_3 and $CaCO_3$ were found to form on the glass surface [31]. The $CaCO_3$ is undesired, as it is inactive towards soot oxidation. By removing calcium, such precipitates are eliminated and any associated catalytically inactive surface regions are removed.

The high temperature resistance to activity degradation occurs from the stronger chemical bonding in the silicate matrix due to the inclusion of network forming elements Ce and Zr. These elements in the glass allow the stabilization of the K in the glass while also resisting the formation of a less active hydrated silicate layer indicative of potash-lime glasses [44,45]. The K ion exchange with adsorbed H_2O on the surface causes a contraction of the surface, essentially shielding the surface from further chemical degradation [44]. Relaxation of the silicate surface further protects the inner glass from extended corrosion in the KCS-1 composition [56–58]. At higher hydrothermal temperatures such as 600 and 700 °C, the KCS-1 glass experienced greater precipitate surface coverage of carbonates (Figure 3). During an active DPF regeneration, the temperature in the rear half of the filter can easily reach 600–700 °C at relatively high soot loads [59,60]. The improved chemical durability of the KCeSZ-1 glass would resist the catalytic degradation imposed upon the catalyst from these high temperature excursions compared to the KCS-1 composition. This would both extend the catalyst lifetime and improve the filter regeneration performance over the full useful lifetime.

Characterization of the hydrothermally derived precipitates seen on the surface of the KCeSZ-1 glass was performed by ATR-FTIR. Figure 4 shows the measured spectra of the KCeSZ-1 glasses after 300, 500, 600, and 700 °C 2 h hydrothermal treatments.

ATR-FTIR spectroscopy of the as-made polished KCeSZ-1 glass revealed peaks at 735 and 872 cm^{-1}. The peak at 735 represent the symmetric Si–O–Si stretching of bridging oxygen atoms, while the peak at 872 cm^{-1} corresponds to the out-of-plane bending in carbonate CO_3^{2-} groups [61–63]. Due to the durability of this composition, there was minimal difference in spectra measured after the 2 h exposures. Only hydrothermal treatments at 300 and 500 °C created a high enough concentration of surface precipitates to yield a discernable change from the as made glass. In these two spectra, small peaks measured at 1398 and 1558 cm^{-1} can be attributed to carbonate formation as has been previously seen [31,61,62]. SEM/EDS analysis confirms these precipitates as potassium rich and thus can be determined to be K_2CO_3.

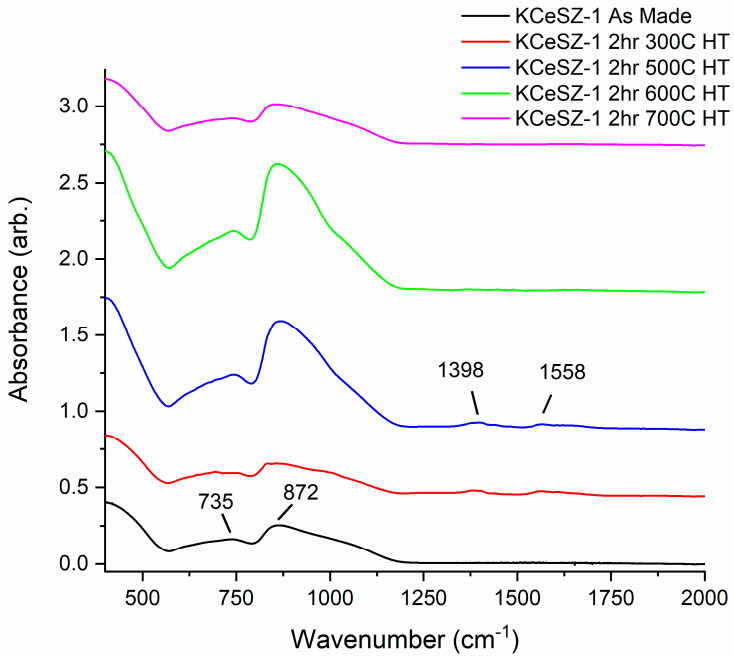

Figure 4. ATR-FTIR spectra of KCeSZ-1 glasses exposed to 2 h hydrothermal treatments in air at temperatures between 300 and 700 °C.

Replacing the Ca in the K-glass composition with Ce and Zr maintained the stability of the glass to hydrothermal degradation and also eliminated the formation of inactive Ca-based precipitates on the glass surface. Cerium as a glass constituent acts as a stronger network former than Ca due to the higher $\Delta G_{hydration}$ of −22.0 kJ/mol [37]. By substituting Ce one not only enhances stability but also introduces an ion that can be catalytically active for soot oxidation.

Ceria-based catalysts for soot oxidation have been recently reviewed [64,65]. In crystalline compounds it is thought that the addition of Zr to Ce enhances thermal stability and may promote the creation of oxygen vacancies/defects in the ceria lattice, improving the oxygen storage capacity and redox properties of ceria [66]. It is not clear if Ce and Zr act synergistically as in crystalline compounds [67], although both Ce and Zr help to stabilize the silica network. K promoted Ce-Zr catalysts have been reported [68,69]. In a series of M-Ce-Zr (M = Mn, Cu, Fe, K, Ba, Sr), catalysts, K-Ce-Zr had the highest catalytic activity under loose contact condition, which was suggested to be due to improvement of the soot-catalyst contact [68]. Neyertz, et al. investigated potassium-promoted $Ce_{0.65}Zr_{0.35}O_2$ catalysts [69]. K/$Ce_{0.65}Zr_{0.35}O_2$/cordierite deactivation was observed after ten cycles of soot combustion.

The catalytic activity of Ce additions to glasses has recently been the focus of interest in the field of biological glasses, where it was shown Ce-containing bioactive glasses inhibit oxidative stress (reduction of hydrogen peroxide), by mimicking the catalase enzyme activity [70–72]. Of direct relevance for the present study of soot oxidation are studies of the local structure around cerium ions in bioactive glasses [73]. The Ce environment in a glass matrix will determine the activity of the material, as it depends on the ability of Ce ions to reversibly change their oxidation state between 3^+ and 4^+. For example, many bioglasses contain phosphorus, which can bind to cerium ions forming cerium phosphate, stabilizing the 3^+ oxidation state and leading to lower catalase activity than phosphorous free glasses [71,74]. Barring any effects from Zr, the KCeSZr-1 glass developed for soot oxidation is chemically similar to the bioglasses studied by Benedetti [73], so it is likely the Ce ions also can reversibly change oxidation state between 3^+ and 4^+ as in crystalline soot catalysts.

3. Materials and Methods

Sol gel powder synthesis, dip coating of cordierite filter slices, and bulk glass slices synthesized by high temperature melting were used to investigate the effects compositional changes on the catalytic soot oxidation activity and hydrothermal durability. In previous testing, a K-Ca-Si-O glass (52 wt% SiO_2, 35 wt% K_2O, 13 wt% CaO (~At%: 47% Si, 40% K, 13% Ca)) was determined to be a promising catalyst [29,32,75]. This composition will be referred to as KCS-1. This composition was taken as the basis for further modification by Zr and Ce substitutions.

For sol gel synthesis of the KCS-1 glass composition (52 wt% SiO_2, 35 wt% K_2O, 13 wt% CaO (~at%: 47% Si, 40% K, 13% Ca)), tetraethylorthosilicate (TEOS) ($Si(OC_2H_5)_4$, 98%), calcium nitrate tetrahydrate ($Ca(NO_3)_2.4H_2O$, ACS reagent) and potassium nitrate (KNO_3, ACS reagent) were used as starting materials, following a well-known approach [76]. TEOS was dissolved in ethanol. Calcium nitrate and potassium nitrate were dissolved in DI water and added to the TEOS-ethanol mixture.

Sols were created for the Ce-Zr containing compositions by using $Ce(NO_3)_3{\cdot}6H_2O$ (98% Alfa Aesar, Haverhill, MA, USA) and Zirconium(IV) isopropanol ispropoxide complex (Alfa Aesar, Haverhill, MA, USA) as precursors for Ce and Zr. Glacial acetic acid (J.T. Baker-Avantor, Radnor, PA, USA) was added to Zr to act as a chelating agent to slow the zirconium condensation reaction and thus elongate the gelation time [77,78]. Isopropanol (70% *v*/*v* in H_2O, Ricca Chemical, Arlington, TX, USA) was added to this separate mixture. The stabilized Zr solution was then added dropwise to the TEOS sol before the addition of the nitrate precursor solution. The excess nitrates compared to the total KCS-1 nitrate amount, added by the Ce precursors, was stabilized in the sol by the addition of equivalent molar amounts of excess 10 wt% malic acid. In this manner, the sol was properly stabilized.

Cordierite filter slices (8 × 8 × 3 mm ($l \times w \times h$)) were vacuum dip coated once the sol reached 10 cP. 10 cP was chosen as the coating viscosity to produce a thin glass film of ~2 μm. This sample size and mass is compatible with the TGA for catalytic activity characterization. Excess sol was blown off with gently flowing air. The coated cordierite slices were aged at 60 C for 24 h in a capped vial, dried at 90 C for an additional 24 h in a capped vial, and then heated to 615 °C in air and held for 1 h, followed by a 10 min hold at 650 °C before cooling to room temperature. During the high temperature stages, remaining nitrates are decomposed. A consistent 5 wt% catalyst loading was achieved through this method. For powder samples, after gelation was complete at 25 °C the gels were heated slowly up to 600 °C over 10 h, held for 1 h, heated to 650 C, held for 15 mins, and cooled to 25 °C. The samples were then crushed by mortar and pestle.

Bulk samples of the KCS-1 and KCeSZ-1 glasses were synthesized by high temperature melting of the oxide components. K_2CO_3, $CaCO_3$, CeO_2, SiO_2, and ZrO_2 (98% Alfa Aesar, Haverhill, MA, USA) were mixed in stoichiometric amounts by mortar and pestle. The glass was then created by heating the mixture to 1400 °C for 6 h followed by subsequent furnace cooling, similar to the process described previously [29,42]. An excess 4 mol% K was added to the precursor mixture to compensate for K volatilization losses K during the high temperature melting process. The bulk melt glass was then cut into 8 × 5 × 3 mm (length × width × height) samples and polished using SiC and Al_2O_3 pads (SiC: 180, 600 grit; Al_2O_3: 12, 3, 0.5 μm). These samples were then dry polished (i.e., polishing without H_2O or other medium to ensure no leaching of K) to a scratch free surface.

Initial tailoring of the K-glass composition was performed by substituting Zr for Ca up to the 2% Zr limit suggested by Cailleteau, et al. [51] in the KCS-1 composition. Ce additions were also made in order to eliminate Ca, and allow for additional K while still keeping $\Delta G_{hydration}$ at a reasonably stable level. The compositions considered are shown in Table 3.

Table 3. Synthesized glass compositions.

Composition	Si	K	Ca	Ce	Zr	ΔG_{hyd} (kJ/mol)
KCS-1	47	40.4	12.6	0	0	−40.4
KCeSZ-1	45	45	0	8	2	−31.6
KCeSZ-2	43.7	44.7	0	9.71	1.94	−31.90
KCeSZ-3	42.06	44.9	0	11.2	1.87	−34.07

Catalytic activity was assessed for the as-made coated cordierite samples by thermogravimetric analysis using a TA Instruments 2950 high resolution thermogravimetric analyzer (HR-TGA, TA Instruments, New Castle, DE, USA). The TGA was programmed to slow the heating ramp rate from 20 °C/min to 2 °C/min when the onset of weight loss was detected. Catalysts were characterized by the soot ignition temperature (T_{ig}) and the 50% soot conversion temperature (T_{50}). A mixed diesel exhaust gas analogue of composition 10% O_2, 5% CO_2, 3% H_2O with balance N_2 was used. Any activity degradation, whether it is due to hydrothermal surface modification or a loss of active potassium, will be detected as an increase in the soot oxidation temperature. To closely mimic the real conditions experienced by a DPF on a diesel engine, "loose" soot contact was achieved by a flame soot deposition technique as described elsewhere [31,79]. Klearol® white mineral oil with ~1 ppm sulfur was used as the fuel oil for soot generation. This fuel was chosen to mitigate any degradation effects that might result from sulfate formation. The soot collection time was controlled to result in a 10:1 catalyst to soot ratio.

For powders, catalytic activity was also characterized using the TGA as described above. Typically, approximately 0.5 mg of soot was combusted in each run with 5.0 mg of catalyst (10:1 catalyst/soot ratio). This is a low enough soot mass to avoid thermal runaway concerns. Both loose (gentle shaking of soot/catalyst mixture in a small vial) and tight (mixing soot and catalyst by mortar and pestle) contact conditions were examined.

Hydrothermal (chemical) degradation was studied on bulk, polished glass samples exposed to humidified gas at temperatures between 300–700 °C. Flowing air (120 mL/min) was bubbled through a heated water bath (40 °C) to accumulate ~7% H_2O vapor before it was fed into a quartz tube furnace which housed the filter samples. The 7% H_2O content was chosen to approximate the diesel exhaust environment [80]. Hydrothermal tests were conducted for 2 h before the catalytic activity was characterized by TGA.

Flat glass slices of the bulk glass samples were used for scanning electron microscopy observations and surface characterization. Structural and chemical changes near the surface (~1–2 μm) were characterized by SEM-EDS and attenuated total reflectance Fourier transform infrared spectroscopy (ATR-FTIR). SEM-EDS analysis was performed on a Carl Zeiss LEO EVO-50 with an Oxford INCA energy dispersive spectrometer (Thornwood, NY, USA). ATR-FTIR was performed on a Bruker Tensor 27 FTIR (Ettlingen, DE) with a platinum single reflection diamond ATR module.

4. Conclusions

The hydrothermal stability of K-Ca-Si-O glass soot oxidation catalysts in a diesel exhaust environment can be improved by considering the field strengths and partial molar free energies of the hydration reactions (ΔG_i) of the cation species in the glass. Substituting Zr and Ce for Ca in a K-Ca-Si-O glass resulted in a diesel soot catalyst with improved hydrothermal stability. The catalytic soot oxidation activity measured by TGA of the KCeSZ-1 glass composition supported on cordierite filter slices compared equally active with the KCS-1 baseline glass composition. As-made soot oxidation temperatures were 390 and 405 °C for T_{ig} and T_{50} respectively. After 2 h 700 °C hydrothermal exposure in air with 7% H_2O, a K-Ca-Si-O glass with a soot T_{50} of 394 °C was found to degrade to 468 °C, whereas the improved K-Ce-Zr-Si-O glass only changed from 407 °C to 427 °C after the same treatment. The K-Ce-Zr-Si-O glass samples showed much improved durability over the K-Ca-Si-O glass, with less formation of precipitates on polished glass surfaces.

Supplementary Materials: The following are available online at http://www.mdpi.com/2073-4344/9/8/684/s1, Table S1. EDS Measured Composition of KCeSZ-1 Glass Surface after 2 h Hydrothermal Exposures at Various Temperatures.

Author Contributions: Conceptualization, C.S. and P.J.M.; Formal analysis, J.Z., C.S. and P.J.M.; Investigation, J.Z. and X.F.; Methodology, C.S.; Supervision, P.J.M.; Writing—original draft, J.Z.; Writing—review & editing, J.Z., X.F., C.S. and P.J.M.

Funding: This research received no external funding.

Acknowledgments: The authors are grateful for use of the XRF facilities through the Center for Environmental Science and Technology (CEST) at University of Notre Dame. SEM characterization was performed through the Notre Dame Integrated Imaging Facility. J.Z. acknowledges partial support of this work through a Bayer graduate fellowship.

Conflicts of Interest: The authors declare there are no conflict of interest.

References

1. di Sarli, V.; Landi, G.; Lisi, L.; di Benedetto, A. Ceria-Coated Diesel Particulate Filters for Continuous Regeneration. *AICHE J.* **2017**, *63*, 3442–3449. [CrossRef]
2. Yuan, S.B.; Meriaudeau, P.; Perrichon, V. Catalytic Combustion of Diesel Soot Particles on Copper—Catalysts Supported on TiO_2—Effect of Potassium Promoter on the Activity. *Appl. Catal. B Environ.* **1994**, *3*, 319–333. [CrossRef]
3. Serra, V.; Saracco, G.; Badini, C.; Specchia, V. Combustion of carbonaceous materials by Cu-K-V based catalysts: 2. Reaction mechanism. *Appl. Catal. B Environ.* **1997**, *11*, 329–346. [CrossRef]
4. Querini, C.A.; Ulla, M.A.; Requejo, F.; Soria, J.; Sedran, U.A.; Miro, E.E. Catalytic combustion of diesel soot particles. Activity and characterization of Co/MgO and Co,K/MgO catalysts. *Appl. Catal. B Environ.* **1998**, *15*, 5–19. [CrossRef]
5. Teraoka, Y.; Kanada, K.; Kagawa, S. Synthesis of La-K-Mn-O perovskite-type oxides and their catalytic property for simultaneous removal of NOx and diesel soot particulates. *Appl. Catal. B Environ.* **2001**, *34*, 73–78. [CrossRef]
6. Liu, J.; Zhao, Z.; Xu, C.M.; Duan, A.; Zhu, L.; Wang, X.Z. Diesel soot oxidation over supported vanadium oxide and K-promoted vanadium oxide catalysts. *Appl. Catal. B Environ.* **2005**, *61*, 36–46. [CrossRef]
7. Aneggi, E.; de Leitenburg, C.; Dolcetti, G.; Trovarelli, A. Diesel soot combustion activity of ceria promoted with alkali metals. *Catal. Today* **2008**, *136*, 3–10. [CrossRef]
8. Li, Q.; Wang, X.; Chen, H.; Xin, Y.; Tian, G.K.; Lu, C.X.; Zhang, Z.L.; Zheng, L.R.; Zheng, L. K-supported catalysts for diesel soot combustion: Making a balance between activity and stability. *Catal. Today* **2016**, *264*, 171–179. [CrossRef]
9. Liu, T.Z.; Li, Q.; Xin, Y.; Zhang, Z.L.; Tang, X.F.; Zheng, L.R.; Gao, P.X. Quasi free K cations confined in hollandite-type tunnels for catalytic solid (catalyst)-solid (reactant) oxidation reactions. *Appl. Catal. B Environ.* **2018**, *232*, 108–116. [CrossRef]
10. Jakubek, T.; Kaspera, W.; Legutko, P.; Stelmachowski, P.; Kotarba, A. How to Efficiently Promote Transition Metal Oxides by Alkali towards Catalytic Soot Oxidation. *Top. Catal.* **2016**, *59*, 1083–1089. [CrossRef]
11. Legutko, P.; Jakubek, T.; Kaspera, W.; Stelmachowski, P.; Sojka, Z.; Kotarba, A. Strong Enhancement of deSoot Activity of Transition Metal Oxides by Alkali Doping: Additive Effects of Potassium and Nitric Oxide. *Top. Catal.* **2017**, *60*, 162–170. [CrossRef]
12. Meloni, E.; Palma, V.; Vaiano, V. Optimized microwave susceptible catalytic diesel soot trap. *Fuel* **2017**, *205*, 142–152. [CrossRef]
13. Rinkenburger, A.; Toriyama, T.; Yasuda, K.; Niessner, R. Catalytic Effect of Potassium Compounds in Soot Oxidation. *ChemCatChem* **2017**, *9*, 3513–3525. [CrossRef]
14. Janiak, C.; Hoffmann, R.; Sjovall, P.; Kasemo, B. The Potassium Promoter Function in the Oxidation of Graphite—An Experimental and Theoretical-Study. *Langmuir* **1993**, *9*, 3427–3440. [CrossRef]
15. Fino, D.; Russo, N.; Saracco, G.; Speechia, V. The role of suprafacial oxygen in some perovskites for the catalytic combustion of soot. *J. Catal.* **2003**, *217*, 367–375. [CrossRef]
16. Li, Q.; Wang, X.; Xin, Y.; Zhang, Z.L.; Zhang, Y.X.; Hao, C.; Meng, M.; Zheng, L.R.; Zheng, L. A unified intermediate and mechanism for soot combustion on potassium-supported oxides. *Sci. Rep.* **2014**, *4*, 4725. [CrossRef] [PubMed]

17. Jelles, S.J.; van Setten, B.; Makkee, M.; Moulijn, J.A. Molten salts as promising catalysts for oxidation of diesel soot: Importance of experimental conditions in testing procedures. *Appl. Catal. B Environ.* **1999**, *21*, 35–49. [CrossRef]
18. McKee, D.W.; Chatterji, D. Catalytic Behavior of Alkali-Metal Carbonates and Oxides in Graphite Oxidation Reactions. *Carbon* **1975**, *13*, 381–390. [CrossRef]
19. McKee, D.W. Gasification of Graphite in Carbon-Dioxide and Water-Vapor—The Catalytic Effects of Alkali-Metal Salts. *Carbon* **1982**, *20*, 59–66. [CrossRef]
20. Kimura, R.; Elangovan, S.P.; Ogura, M.; Ushiyama, H.; Okubo, T. Alkali Carbonate Stabilized on Aluminosilicate via Solid Ion Exchange as a Catalyst for Diesel Soot Combustion. *J. Phys. Chem. C* **2011**, *115*, 14892–14898. [CrossRef]
21. Grzona, C.B.; Lick, I.D.; Castellon, E.R.; Ponzi, M.I.; Ponzi, E.N. Cobalt and KNO_3 supported on alumina catalysts for diesel soot combustion. *Mater. Chem. Phys.* **2010**, *123*, 557–562. [CrossRef]
22. Miyazaki, T.; Tokubuchi, N.; Arita, M.; Inoue, M.; Mochida, I. Catalytic combustion of carbon by alkali metal carbonates supported on perovskite-type oxide. *Energy Fuels* **1997**, *11*, 832–836. [CrossRef]
23. Teraoka, Y.; Nakano, K.; Kagawa, S.; Shangguan, W.F. Simultaneous Removal of Nitrogen-Oxides and Diesel Soot Particulates Catalyzed by Perovskite-Type Oxides. *Appl. Catal. B Environ.* **1995**, *5*, L181–L185. [CrossRef]
24. Shangguan, W.F.; Teraoka, Y.; Kagawa, S. Promotion effect of potassium on the catalytic property of CuFe2O4 for the simultaneous removal of NOx and diesel soot particulate. *Appl. Catal. B Environ.* **1998**, *16*, 149–154. [CrossRef]
25. Milt, V.G.; Pissarello, M.L.; Miro, E.E.; Querini, C.A. Abatement of diesel-exhaust pollutants: NOx storage and soot combustion on K/La_2O_3 catalysts. *Appl. Catal. B Environ.* **2003**, *41*, 397–414. [CrossRef]
26. Hizbullah, K.; Kureti, S.; Weisweiler, W. Potassium promoted iron oxide catalysts for simultaneous catalytic removal of nitrogen oxides and soot from diesel exhaust gas. *Catal. Today* **2004**, *93–95*, 839–843. [CrossRef]
27. Peralta, M.A.; Milt, V.G.; Cornaglia, L.M.; Querini, C.A. Stability of $Ba,K/CeO_2$ catalyst during diesel soot combustion: Effect of temperature, water, and sulfur dioxide. *J. Catal.* **2006**, *242*, 118–130. [CrossRef]
28. Moggia, J.M.; Milt, V.G.; Ulla, M.A.; Cornaglia, L.M. Surface characterization of $Co,K/La_2O_3$ catalysts used for the catalytic combustion of diesel soot. *Surf. Interface Anal.* **2003**, *35*, 216–225. [CrossRef]
29. An, H.M.; Su, C.S.; McGinn, P.J. Application of potash glass as a catalyst for diesel soot oxidation. *Catal. Commun.* **2009**, *10*, 509–512. [CrossRef]
30. Su, C.S.; McGinn, P.J. Application of glass soot catalysts on metal supports to achieve low soot oxidation temperature. *Catal. Commun.* **2014**, *43*, 1–5. [CrossRef]
31. Zokoe, J.; McGinn, P.J. Catalytic diesel soot oxidation by hydrothermally stable glass catalysts. *Chem. Eng. J.* **2015**, *262*, 68–77. [CrossRef]
32. Zokoe, J.; Su, C.; McGinn, P.J. Soot Combustion Activity and Potassium Mobility in Diesel Particulate Filters Coated with a K–Ca–Si–O Glass Catalyst. *Ind. Eng. Chem. Res.* **2019**, *58*, 11891–11901. [CrossRef]
33. Su, C.S.; McGinn, P.J. The effect of Ca^{2+} and Al^{3+} additions on the stability of potassium disilicate glass as a soot oxidation catalyst. *Appl. Catal. B Environ.* **2013**, *138*, 70–78. [CrossRef]
34. Lopez-Suarez, F.E.; Bueno-Lopez, A.; Illan-Gomez, M.J.; Ura, B.; Trawczynski, J. Potassium Stability in Soot Combustion Perovskite Catalysts. *Top. Catal.* **2009**, *52*, 2097–2100. [CrossRef]
35. Neyertz, C.A.; Miro, E.E.; Querini, C.A. K/CeO_2 catalysts supported on cordierite monoliths: Diesel soot combustion study. *Chem. Eng. J.* **2012**, *181*, 93–102. [CrossRef]
36. White, W.B. Theory of Corrosion of Glass and Ceramics. In *Corrosion of Glass, Ceramics, and Ceramic Superconductors: Principles, Testing, Characterization and Applications*; Clark, D.E., Zoitos, B.K., Eds.; Noyes Publications: Park Ridge, NJ, USA, 1992; pp. 2–28.
37. Perret, D.; Crovisier, J.L.; Stille, P.; Shields, G.; Mader, U.; Advocat, T.; Schenk, K.; Chardonnens, M. Thermodynamic stability of waste glasses compared to leaching behavior. *Appl. Geochem.* **2003**, *18*, 1165–1184. [CrossRef]
38. Silva, A.C.; Mello-Castanho, S.R.H. Vitrified galvanic waste chemical stability. *J. Eur. Ceram. Soc.* **2007**, *27*, 565–570. [CrossRef]
39. Melcher, M.; Wiesinger, R.; Schreiner, M. Degradation of Glass Artifacts: Application of Modern Surface Analytical Techniques. *Acc. Chem. Res.* **2010**, *43*, 916–926. [CrossRef]
40. Newton, R.G. The Durability of Glass—A Review. *Glass Technol.* **1985**, *26*, 21–38.

41. Gentaz, L.; Lombardo, T.; Loisel, C.; Chabas, A.; Vallotto, M. Early stage of weathering of medieval-like potash-lime model glass: Evaluation of key factors. *Environ. Sci. Pollut. Res.* **2011**, *18*, 291–300. [CrossRef]
42. An, H.M.; Kilroy, C.; McGinn, P.J. Combinatorial synthesis and characterization of alkali metal doped oxides for diesel soot combustion. *Catal. Today* **2004**, *98*, 423. [CrossRef]
43. Miyazaki, T.; Tokubuchi, N.; Inoue, M.; Arita, M.; Mochida, I. Catalytic activities of K_2CO_3 supported on several oxides for carbon combustion. *Energy Fuels* **1998**, *12*, 870–874. [CrossRef]
44. Paul, A. Chemical Durability of Glasses—Thermodynamic Approach. *J. Mater. Sci.* **1977**, *12*, 2246–2268. [CrossRef]
45. Jantzen, C.M. Thermodynamic Approach to Glass Corrosion. In *Corrosion of Glass, Ceramics, and Ceramic Superconductors: Principles, Testing, Characterization and Applications*; Clark, D.E., Zoitos, B.K., Eds.; Noyes Publications: Park Ridge, NJ, USA, 1992; pp. 153–217.
46. McKee, D.W. The Catalyzed Gasification Reactions of Carbon. *Chem. Phys. Carbon* **1981**, *16*, 1–118.
47. Sato, K.; Yamaguchi, M.; Fujita, S.; Suzuki, K.; Mori, T. Enhancement of the activity of calcium aluminosilicate ($Ca1_2Al1_0Si_4O_{35}$) for the combustion of diesel soot via the substitution of Ca^{2+} ions with transition metal ions. *Catal. Commun.* **2006**, *7*, 132–135. [CrossRef]
48. Das, C.R. Chemical Durability of Sodium-Silicate Glasses Containing Al_2O_3 and ZrO_2. *J. Am. Ceram. Soc.* **1981**, *64*, 188–193. [CrossRef]
49. Karell, R.; Kraxner, J.; Chromcikova, M. Properties of selected, zirconia containing silicate glasses. *Ceram. Silik.* **2006**, *50*, 78–82.
50. Stanova, I.; Plsko, A.; Pagacova, J.; Sibikova, K. Influence of composition on corroding process of Na2O-K2O-CaO-ZrO2-SiO2 glasses. *Chem. Pap.* **2007**, *61*, 11–15. [CrossRef]
51. Cailleteau, C.; Angeli, F.; Devreux, F.; Gin, S.; Jestin, J.; Jollivet, P.; Spalla, O. Insight into silicate-glass corrosion mechanisms. *Nat. Mater.* **2008**, *7*, 978–983. [CrossRef]
52. Sajeevan, A.C.; Sajith, V. A study on Oxygen Storage capacity of Zirconium-Cerium-Oxide Nanoparticles. In *Advanced Materials Research Iii*; Gupta, K.M., Ed.; Trans Tech Publications Ltd.: Stafa-Zurich, Switzerland, 2013; pp. 123–127.
53. Zhang, J.; Kumagai, H.; Yamamura, K.; Ohara, S.; Takami, S.; Morikawa, A.; Shinjoh, H.; Kaneko, K.; Adschiri, T.; Suda, A. Extra-Low-Temperature Oxygen Storage Capacity of CeO_2 Nanocrystals with Cubic Facets. *Nano Lett.* **2011**, *11*, 361–364. [CrossRef]
54. Zhang, Y.; Andersson, S.; Muhammed, M. Nanophase Catalytic Oxides. 1. Synthesis of Doped Cerium Oxides as Oxygen Storage Promoters. *Appl. Catal. B Environ.* **1995**, *6*, 325–337. [CrossRef]
55. Miceli, P.; Bensaid, S.; Russo, N.; Fino, D. CeO_2-based catalysts with engineered morphologies for soot oxidation to enhance soot-catalyst contact. *Nanoscale Res. Lett.* **2014**, *9*, 254. [CrossRef]
56. Tomozawa, M.; Kim, D.L.; Agarwal, A.; Davis, K.M. Water diffusion and surface structural relaxation of silica glasses. *J. Non-Cryst. Solids* **2001**, *288*, 73–80. [CrossRef]
57. Ingram, M.D.; Wu, M.H.; Coats, A.; Kamitsos, E.I.; Varsamis, C.P.E.; Garcia, N.; Sola, M. Evidence from infrared spectroscopy of structural relaxation during field assisted and chemically driven ion exchange in soda-lime-silica glasses. *Phys. Chem. Glasses* **2005**, *46*, 84–89.
58. Koike, A.; Tomozawa, M. Towards the origin of the memory effect in oxide glasses. *J. Non-Cryst. Solids* **2008**, *354*, 3246–3253. [CrossRef]
59. Neeft, J.P.A.; Makkee, M.; Moulijn, J.A. Diesel particulate emission control. *Fuel Process. Technol.* **1996**, *47*, 1–69. [CrossRef]
60. Yamamoto, K.; Yamauchi, K. Numerical simulation of continuously regenerating diesel particulate filter. *Proc. Combust. Inst.* **2013**, *34*, 3083–3090. [CrossRef]
61. ElBatal, H.A.; Azooz, M.A.; Khalil, E.M.A.; Monem, A.S.; Hamdy, Y.M. Characterization of some bioglass-ceramics. *Mater. Chem. Phys.* **2003**, *80*, 599–609. [CrossRef]
62. Vilarigues, M.; da Silva, R.C. Characterization of potash-glass corrosion in aqueous solution by ion beam and IR spectroscopy. *J. Non-Cryst. Solids* **2006**, *352*, 5368–5375. [CrossRef]
63. Vilarigues, M.; da Silva, R.C. The effect of Mn, Fe and Cu ions on potash-glass corrosion. *J. Non-Cryst. Solids* **2009**, *355*, 1630–1637. [CrossRef]
64. Liu, S.; Wu, X.D.; Weng, D.; Ran, R. Ceria-based catalysts for soot oxidation: A review. *J. Rare Earths* **2015**, *33*, 567–590. [CrossRef]

65. Mahamulkar, S.; Yin, K.H.; Agrawal, P.K.; Davis, R.J.; Jones, C.W.; Malek, A.; Shibata, H. Formation and Oxidation/Gasification of Carbonaceous Deposits: A Review. *Ind. Eng. Chem. Res.* **2016**, *55*, 9760–9818. [CrossRef]
66. Bueno-López, A. Diesel soot combustion ceria catalysts. *Appl. Catal. B Environ.* **2014**, *146*, 1–11. [CrossRef]
67. Wu, X.D.; Liu, D.X.; Li, K.; Li, J.; Weng, D. Role of CeO_2-ZrO_2 in diesel soot oxidation and thermal stability of potassium catalyst. *Catal. Commun.* **2007**, *8*, 1274–1278. [CrossRef]
68. Alinezhadchamazketi, A.; Khodadadi, A.A.; Mortazavi, Y.; Nemati, A. Catalytic evaluation of promoted CeO_2-ZrO_2 by transition, alkali, and alkaline-earth metal oxides for diesel soot oxidation. *J. Environ. Sci.* **2013**, *25*, 2498–2506. [CrossRef]
69. Neyertz, C.A.; Banus, E.D.; Miro, E.E.; Querini, C.A. Potassium-promoted $Ce0.65Zr0.35O_2$ monolithic catalysts for diesel soot combustion. *Chem. Eng. J.* **2014**, *248*, 394–405. [CrossRef]
70. Nicolini, V.; Gambuzzi, E.; Malavasi, G.; Menabue, L.; Menziani, M.C.; Lusvardi, G.; Pedone, A.; Benedetti, F.; Luches, P.; D'Addato, S.; et al. Evidence of Catalase Mimetic Activity in Ce^{3+}/Ce^{4+} Doped Bioactive Glasses. *J. Phys. Chem. B* **2015**, *119*, 4009–4019. [CrossRef]
71. Nicolini, V.; Varini, E.; Malavasi, G.; Menabue, L.; Menziani, M.C.; Lusvardi, G.; Pedone, A.; Benedetti, F.; Luches, P. The effect of composition on structural, thermal, redox and bioactive properties of Ce-containing glasses. *Mater. Des.* **2016**, *97*, 73–85. [CrossRef]
72. Nicolini, V.; Malavasi, G.; Menabue, L.; Lusvardi, G.; Benedetti, F.; Valeri, S.; Luches, P. Cerium-doped bioactive 45S5 glasses: Spectroscopic, redox, bioactivity and biocatalytic properties. *J. Mater. Sci.* **2017**, *52*, 8845–8857. [CrossRef]
73. Benedetti, F.; Luches, P.; D'Addato, S.; Valeri, S.; Nicolini, V.; Pedone, A.; Menziani, M.C.; Malavasi, G. Structure of active cerium sites within bioactive glasses. *J. Am. Ceram. Soc.* **2017**, *100*, 5086–5095. [CrossRef]
74. Leonelli, C.; Lusvardi, G.; Malavasi, G.; Menabue, L.; Tonelli, M. Synthesis and characterization of cerium-doped glasses and in vitro evaluation of bioactivity. *J. Non-Cryst. Solids* **2003**, *316*, 198–216. [CrossRef]
75. Su, C.S. Stabilization of potassium in soot oxidation catalysts and their application on diesel particulate filters. In *Chemical & Biomolecular Engineering*; University of Notre Dame: Notre Dame, IN, USA, 2011.
76. Saravanapavan, P.; Hench, L.L. Mesoporous calcium silicate glasses. I. Synthesis. *J. Non-Cryst. Solids* **2003**, *318*, 1–13. [CrossRef]
77. Wellbrock, U.; Beier, W.; Frischat, G.H. Preparation of SiO_2-TiO_2-ZrO_2 Gel Glasses and Coatings By Means Of Modified Alkoxide Solutions. *J. Non-Cryst. Solids* **1992**, *147*, 350–355. [CrossRef]
78. Avendano, R.G.R.; de los Reyes, J.A.; Montoya, J.A.; Viveros, T. Effect of synthesis parameters on sol-gel silica modified by zirconia. *J. Sol-Gel Sci. Technol.* **2005**, *33*, 133–138. [CrossRef]
79. Su, C.; Wang, Y.; Kumar, A.; McGinn, P. Simulating Real World Soot-Catalyst Contact Conditions for Lab-Scale Catalytic Soot Oxidation Studies. *Catalysts* **2018**, *8*, 247. [CrossRef]
80. Resitoglu, I.A.; Altinisik, K.; Keskin, A. The pollutant emissions from diesel-engine vehicles and exhaust aftertreatment systems. *Clean Technol. Environ. Policy* **2015**, *17*, 15–27. [CrossRef]